



# A novel biosensor based on serum antibody immobilization for rapid detection of viral antigens

Tran Quang Huy<sup>a,b,\*</sup>, Nguyen Thi Hong Hanh<sup>a</sup>, Nguyen Thanh Thuy<sup>a</sup>, Pham Van Chung<sup>a</sup>, Phan Thi Nga<sup>a</sup>, Mai Anh Tuan<sup>b</sup>

<sup>a</sup> National Institute of Hygiene and Epidemiology (NIHE), 1 Yersin Street, Hanoi, Viet Nam

<sup>b</sup> International Training Institute for Materials Science (ITIMS), Hanoi University of Science and Technology (HUST), 1 Dai Co Viet Road, Hanoi, Viet Nam

## ARTICLE INFO

### Article history:

Received 9 August 2011

Received in revised form 9 September 2011

Accepted 9 September 2011

Available online 16 September 2011

### Keywords:

Immunosensor

Serum antibody immobilization

Viral antigen detection

Preliminary pathogenic screening

Outbreak

## ABSTRACT

In this paper, we represent a label-free biosensor based on immobilization of serum antibodies for rapid detection of viral antigens. Human serum containing specific antibodies against Japanese encephalitis virus (JEV) was immobilized on a silanized surface of an interdigitated sensor via protein A/glutaraldehyde for electrical detection of JEV antigens. The effective immobilization of serum antibodies on the sensor surface was verified by Fourier transform infrared spectrometry and fluorescence microscopy. The signal of the biosensor obtained by the differential voltage converted from the change into non-Faradic impedance resulting from the specific binding of JEV antigens on the surface of the sensor. The detection analyzed indicates that the detection range of this biosensor is 1–10 µg/ml JEV antigens, with a detection limit of 0.75 µg/ml and that stable signals are measured in about 20 min. This study presents a useful biosensor with a high selectivity for rapid and simple detection of JEV antigens, and it also proposes the biosensor as a future diagnostic tool for rapid and direct detection of viral antigens in clinical samples for preliminary pathogenic screenings in the case of possible outbreaks.

© 2011 Elsevier B.V. All rights reserved.

## 1. Introduction

Recent years have witnessed an increasing number of emerging and re-emerging infectious diseases caused by viruses such as SARS-Cov, influenza A/H<sub>5</sub>N<sub>1</sub>, influenza A/H<sub>1</sub>N<sub>1</sub>, Dengue virus, HIV, and new encephalitis viruses; they are likely to break out into highly infectious diseases endangering public health, and to lead to increased numbers of persons infected in a short period of time [1,2]. Most individuals presenting similar symptoms of certain infectious diseases should normally be isolated or sent to hospitals even though the diagnosis of not all of them leads to the same positive results. Consequently, hospitals can become overloaded, and many patients could receive inappropriate treatments and/or become co-infected. Therefore, early diagnostic tests and preliminary pathogenic screening are crucial for the control and prevention of these diseases as well as for the treatments of patients in outbreaks [3]. Several conventional laboratory diagnostic methods have been applied to confirm the identity of the pathogen such as serology (immunofluorescence techniques, neutralization tests

and enzyme-linked immunosorbent assay (ELISA), etc.), indirect or direct examination (inoculation, animal tests, electron microscopy, antigen detection, molecular techniques (PCR), etc.) [4]. However, these diagnostic techniques require a pre-treated sample, biological products, standard biosafe laboratories and time-consuming analyses to yield a reliable answer. In recent decades, biosensors/biochips have been envisaged to compensate and complement conventional diagnostic methods due to their easy operation and transport; they require no reagent and provide results in a few minutes [5–7]. There are two main kinds of biosensors for pathogen detection, based on the hybridization of oligonucleotides (DNA sensors or oligonucleotide-based biosensors) [8,9], and on the specific reaction of antibody–antigen (immunosensors or antibody-based biosensors) [10]. Oligonucleotide-based biosensors are ultrasensitive diagnostic devices which can use the simple impedance measurements [11] or scanning electrochemical microscopy [12,13] for oligonucleotide hybridization and mismatch detection. However, their limitations in virus detection result from the design of probe molecules, and the complexity of extraction and denaturation of viral DNA or RNA [14]. Antibody-based biosensors have become more useful, and most of the biosensors developed are designed based on electrochemical, optical or micro-gravimetric detection [15–18]. Among them, biosensors based on electrical/electrochemical detection have the advantage of being highly sensitive, rapid, inexpensive and highly

\* Corresponding author at: National Institute of Hygiene and Epidemiology (NIHE), 1 Yersin Street, Hanoi, Viet Nam. Tel.: +84 4 39 71 54 34; fax: +84 4 38 21 08 53; mobile: +84 9 78 96 06 58.

E-mail address: [huytq@nihe.org.vn](mailto:huytq@nihe.org.vn) (T.Q. Huy).

amenable to micro-fabrication, and it is also easy to measure the changes in electrical/electrochemical properties resulting from biochemical reactions on the surface of the sensor [19,20]. For pathogen detection, biosensors based on micro-electrode fingers maximize the impedance change at the surface of the micro-electrode array, and not throughout the test sample [21]. This allows for the biosensor to detect pathogen in solution with minimal effects of other components in the sample. Furthermore, micro-electrodes also have great advantages over conventional electrodes for analytical measurements due to the high signal-to-noise ratio, the use of small volumes, low resistance and rapid attainment of steady state; thus micro-electrode-based sensors have received great attention in impedimetric immunosensing and biosensing [22]. However, most of biosensors normally use purified or labeled antibodies to detect viral antigens [23–25]. In outbreaks, it is not easy to dispose of specific antibodies (purified antibodies) against these pathogens, especially against unknown pathogens within a short period of time, and screened human serum becomes an effective choice to develop serum antibody-based biosensors for preliminary pathogen screening.

In this paper, a label-free biosensor has been developed based on the immobilization of serum antibodies and non-Faradic impedance for rapid detection of Japanese encephalitis virus (JEV) antigens. The use of interdigitated sensors designed with two separate micro-electrode regions of the working and reference electrodes was convenient for electrical measurements, and the change in impedance caused by the binding of viral antigens to the sensor surface resulting in the difference of the voltage between these two electrodes. Furthermore, protein A was also used as an effective intermediate linker in order to bind and orient serum antibodies on the sensor surface for optimal detection.

## 2. Materials and methods

### 2.1. Reagents and electrochemical sensors

Human serum containing antibodies against JEV (tested for non-cross reactivity with other *flaviviruses* and Hepatitis B virus), inactivated JEV (JEV antigens), Dengue virus (Dengue antigens), and healthy mouse serum were provided by the Laboratory of Arboviruses, National Institute of Hygiene and Epidemiology (NIHE) of Vietnam. These biological products were stored at  $-20^{\circ}\text{C}$  before use.

Fluorescein isothiocyanate (FITC)-conjugated mouse anti-human IgG antibodies (FITC-Ab), bovine serum albumin (BSA), 3-aminopropyl-triethoxy-silane (APTES), glutaraldehyde (GA) and protein A (PrA) were purchased from Sigma, USA. All other chemicals were of analytical grade.

The interdigitated sensors were designed and fabricated at the Hanoi University of Science and Technology (HUST). The fingers of interdigitated electrodes were  $10\text{ }\mu\text{m}$  wide and their gap size was  $10\text{ }\mu\text{m}$ , by sputtering  $10\text{ nm}$  Ti and  $200\text{ nm}$  Pt on a  $100\text{ nm}$  thermally thick silicon dioxide ( $\text{SiO}_2$ ) layer grown on top of a silicon wafer (Fig. 1). The electrochemical characteristics of this sensor have been investigated and applied in several studies [14,26].

### 2.2. Immobilization of serum antibodies on the sensor surface

Sensors were immersed in a  $1\text{ M}$  KOH/MeOH solution for 30 min for surface cleaning and adequate functioning. They were then rinsed in de-ionized (DI) water and nitrogen-dried. The silanization process was conducted in 5% APTES/MeOH for 1 h to create functional amino groups ( $-\text{NH}_2$ ). A small drop of acetic acid was added during the silanization to orient the amino groups outward of the interdigitated surface. Sensors were then washed three times

with DI water, nitrogen-dried, and annealed thermally at  $120^{\circ}\text{C}$  for 6–8 min to completely remove excess water molecules from the surface. The silanized sensors were kept in a dry box at room temperature until used.

The silanized sensor was dipped in 5% glutaraldehyde for 30 min and washed in DI water three times. Next,  $5\text{ }\mu\text{l}$  of PrA solution [ $1\text{ mg}$  PrA/ml phosphate-buffered saline (PBS; pH 7.0)] was deposited on the surface and incubated for 30 min, then washed in PBS (pH 7.0) followed by incubation in  $1\text{ mg/ml}$  serum containing antibodies against JEV for 1 h. The unsaturated and non-specific binding sites on the surface were blocked with 2% BSA in PBS for 30 min, washed with PBS, and air-dried. All steps of immobilization were performed at room temperature.

### 2.3. Fourier transform infrared spectrometry

Fourier transform infrared (FTIR) spectroscopy (Nicolet 6700 FTIR machine, Thermo, USA) was used to characterize the presence of specific chemical groups as well as the effective binding of proteins (serum antibodies, protein A) on the silanized interdigitated surface before and after the immobilization of serum antibodies and washing steps. To conduct these measurements, FTIR spectra were obtained in the range of  $1800\text{--}1300\text{ cm}^{-1}$  for protein analyses, with 200 scans and  $2\text{ cm}^{-1}$  of resolution. The techniques used to record FTIR absorption spectra of the antibodies on the silanized interdigitated surface were performed following the procedures of Sibai [27].

### 2.4. Fluorescence microscopy

The density and binding efficiency of serum antibodies immobilized on the silanized surface were investigated by fluorescence microscopy (Eclipse 90i, Nikon, Japan). These experiments were carried out on microscope slides with the same protocol as for serum antibody immobilization as applied to the interdigitated biosensor. In this method, FITC-Ab was used to verify the effective binding of human IgG antibodies immobilized on the PrA/GA/silanized surface. The reference test was also conducted using BSA instead of serum antibodies.

### 2.5. Impedance spectroscopy of the serum antibody-based interdigitated sensor

The serum antibody-based interdigitated sensor was immersed into a cell filled with PBS with the absence of JEV antigens. A potential of  $100\text{ mV}$  was applied across the electrodes and measurement of impedance change was performed using an IM6ex impedance analyzer (Germany) with the frequency range from  $1\text{ Hz}$  to  $1\text{ MHz}$ . Bode (impedance versus frequency) diagram was recorded.

### 2.6. Detection of JEV antigens

Electrical measurements were performed at room temperature by immersing the biosensor into a cell filled with PBS, then adding defined concentrations of viral antigens. A potential of  $100\text{ mV}$  with five fixed frequencies of  $100\text{ Hz}$ ,  $1\text{ kHz}$ ,  $10\text{ kHz}$ ,  $100\text{ kHz}$  and  $1\text{ MHz}$  was applied to electrodes using an RS830 Lock-in amplifier (Stanford Research Systems, USA) to determine the best conditions for measurements. The change in impedance caused by the specific interaction between the JEV antigens and serum antibodies on the sensor surface was measured by the difference of the voltage drop across two  $1\text{ k}\Omega$  resistors, between working electrodes and reference electrodes using channels A and B of the Lock-in amplifier and processed by a computer [26]. The non-specific reactions

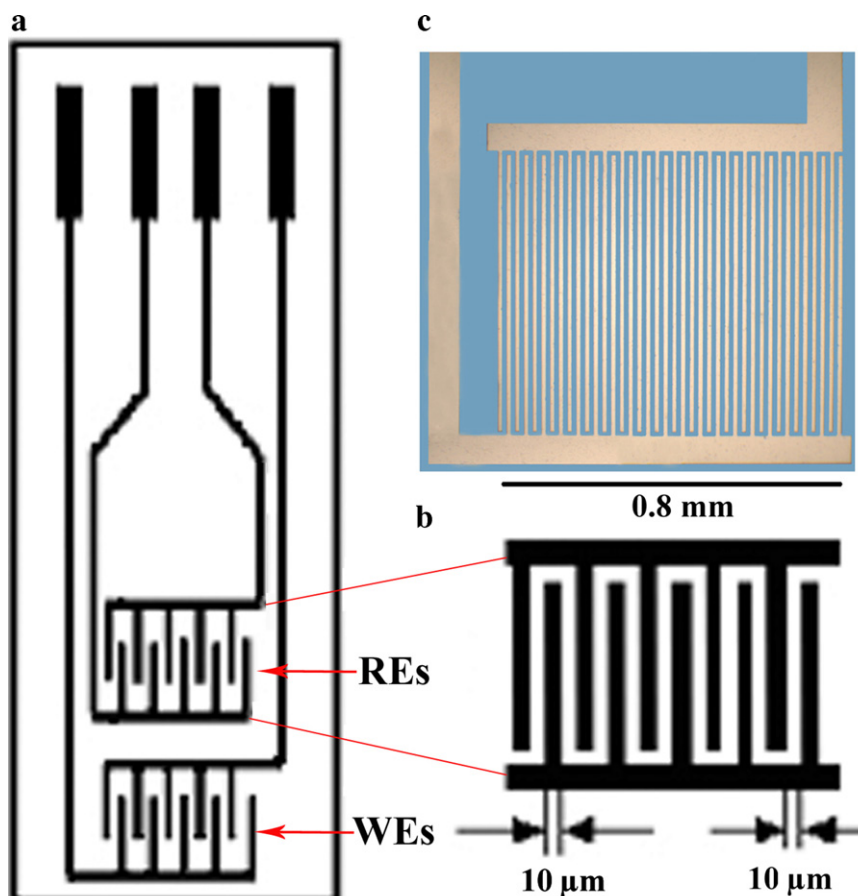


**Fig. 1.** Diagram of an interdigitated sensor with working electrodes (WEs) and reference electrodes (REs) (a), a zoom of electrode finger (b), and a real fabricated electrode area (c).

were tested using a closely related viral antigen—Dengue virus and mouse serum under the same conditions as for JEV antigens.

### 3. Results and discussion

#### 3.1. Characterization of serum antibody immobilization

After immobilizing serum antibodies on the silanized interdigitated surface and after the washing steps, Fourier transform infrared spectroscopy was used to characterize the presence of specific chemical groups as well as the efficient binding of these antibodies on the sensor surface. Fig. 2 shows the FTIR absorption spectra of proteins (serum antibodies and protein A) in the range of  $1800\text{--}1300\text{ cm}^{-1}$ . Previous studies reported that the protein repeat units gave rise to good characteristic infrared absorption bands namely, amide A, amide B, and amides I–VII. Among these absorption bands, those of amides I and II are the most prominent vibrational bands of the protein backbone [28–30]. Fig. 2b shows the highly characteristic peaks of proteins obtained by the serum/PrA/GA/silanized surface corresponding to the peak around  $1640\text{ cm}^{-1}$  of the amide I band with  $\text{C=O}$  stretching frequency, and the peak around  $1550\text{ cm}^{-1}$  of the amide II band with  $\text{C-N}$  stretching and  $\text{N-H}$  bending. The peak of the  $\text{C=O}$  vibration mode is also found at  $1420\text{ cm}^{-1}$  obtained on samples after serum antibody immobilization, but not on the interdigitated surface treated with APTES only (Fig. 2a) [27].

To verify good binding of serum antibodies on the interdigitated surface, FITC-Ab was dropped and incubated on the slides immobilized with BSA and serum antibodies/PrA during 30 min. After

the washing steps, these slides were investigated by fluorescence microscopy. Fig. 3 shows that a density of green fluorescent spots could be observed clearly on the slide surfaces immobilized with serum antibodies/PrA (Fig. 3b) in comparison with blank color of the surface treated with BSA instead of serum antibodies (Fig. 3a). This proved that a large number of serum antibodies could remain and orient well on the sensor surface. In fact, IgG molecules are the main immunoglobulins, constituting 75% of the total immunoglobulins in human serum [31]; they are also major factors responsible for the detection of antigens in immunosensor applications. In these experiments, PrA was used to immobilize serum antibodies on the silanized surface. PrA can bind with high affinity to immunoglobulins, especially to the Fc region of human IgG1 and IgG2, binds with moderate affinity to human IgM, IgA and IgE, but not react with human IgG3, IgD or other proteins in human serum. This binding of PrA to immunoglobulin molecules does not influence their binding sites of the antigen [32]. Moreover, PrA is also often immobilized onto a solid support and used as reliable method for purifying total IgG from crude protein mixtures. This agrees with previous publications reporting that PrA is the best choice for selection and orientation of IgG antibodies with the antigen binding sites outwards from the surface [33–36], and leading to the possibility that antibodies used to capture viral antigens will be increased significantly on the sensor surface.

#### 3.2. The equivalent circuit of the serum antibody-based interdigitated sensor

The surface of interdigitated sensor was functionalized by APTES and protein A, serum antibodies were then immobilized to form a

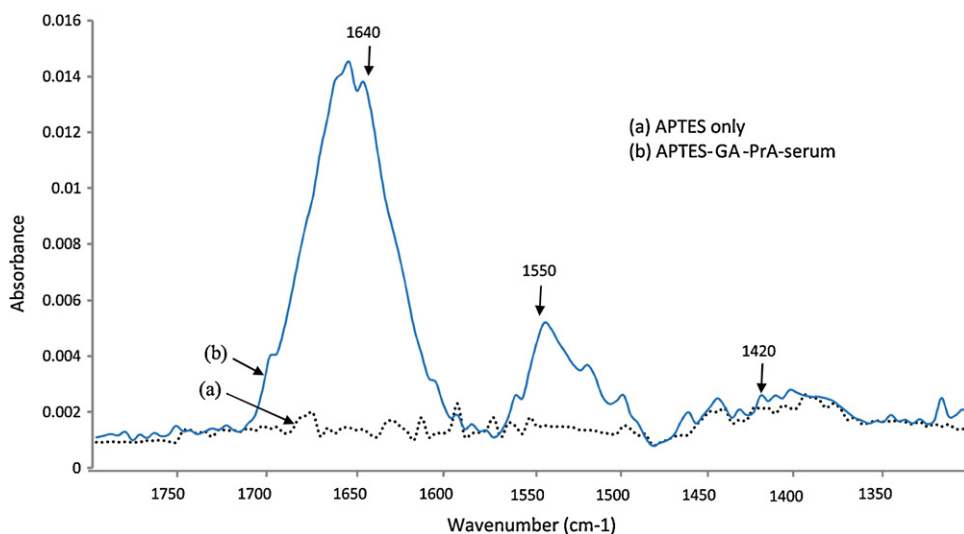


**Fig. 2.** Characteristic FTIR absorption spectrum of interdigitated surfaces before (a) and after the immobilization of serum antibodies with the peaks of proteins, around  $1640\text{ cm}^{-1}$  of amide I and  $1550\text{ cm}^{-1}$  of amide II (b).

biological transducer. When the biosensor was immersed into the solution for measurements, viral antigens become bound to the serum antibodies attached to the sensor surface. This resulted in the change in impedance measured across the electrodes. Fig. 4a describes a simple modified equivalent circuit for viral antigens bound to the sensor surface immobilized with serum antibodies, where the interfacial resistance of the biomolecules complex on the sensor surface ( $R_{cs}$ ) and two identical double layer capacitances ( $C_{dl}$ ) of the two sets of electrodes are connected to the solution resistance ( $R_{sol}$ ) in series, and the dielectric capacitance of the solution ( $C_{di}$ ) [21,37–39]. This circuit model was also interpreted with two parallel branches of the dielectric capacitance and impedance. Fig. 4b shows the impedance spectrum of the serum antibody-based interdigitated sensor in the frequency range from 1 Hz to 1 MHz, with the fitting curve to the equivalent circuit. The fitting curve matched the measured data, validating the equivalent circuit. In this figure, the impedance decreased linearly with the increasing frequency in the range from 1 Hz to around 1.5 kHz, and became independent of the frequency in the range from 1.5 kHz to 1 MHz. At low frequencies (<1.5 kHz) the current does not flow through the solution and the binding of viral antigens to serum antibodies immobilized on the sensor surface add different impedance elements to the change in total impedance. When frequency is sufficiently high (>1 MHz) the dielectric capacitance of the solution dominates the total impedance, and the contribution of double

layer capacitances and solution resistance to total impedance is minimal [21]. According to Yang et al. [39], when the frequency is not sufficiently high (<1 MHz), the current cannot pass through the dielectric capacitor. So, the parallel dielectric capacitance is inactive, and just acts as an open circuit. Only the double layer capacitance and solution resistance in series need to be taken into account for the total impedance, and the role of dielectric capacitance ( $C_{di}$ ) is ignored. Otherwise, Fang et al. [38] reported that the current could flow across the biomolecule layer immobilized on the sensor surface from this electrode to another at low frequencies. In this work, the dielectric capacitance branch was not studied.

### 3.3. Detection of JEV antigens

First, the solution of JEV antigens was checked for the presence of virus particles. By using ultracentrifugation and transmission electron microscopy, JEV particles with spherical shapes and about 45 nm in diameter were detected in the sample (Fig. 5b). The biosensors were then immersed in different concentrations of JEV antigens diluted in PBS for measurements. Fig. 5a shows the differential impedances changed by the reaction of serum antibodies and various concentrations of JEV antigens on the sensor surface at a frequency of 1 kHz after 20 min of incubation. These data were calculated from the differential voltage in the output signals between the working and reference electrodes, using channels

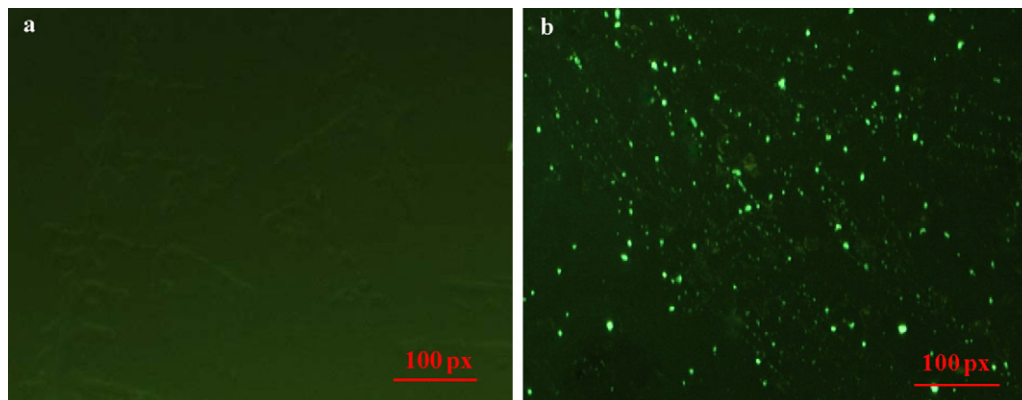


**Fig. 3.** Fluorescence images of FITC-Abs on microscope slides immobilized with BSA (a) and serum antibodies (b).

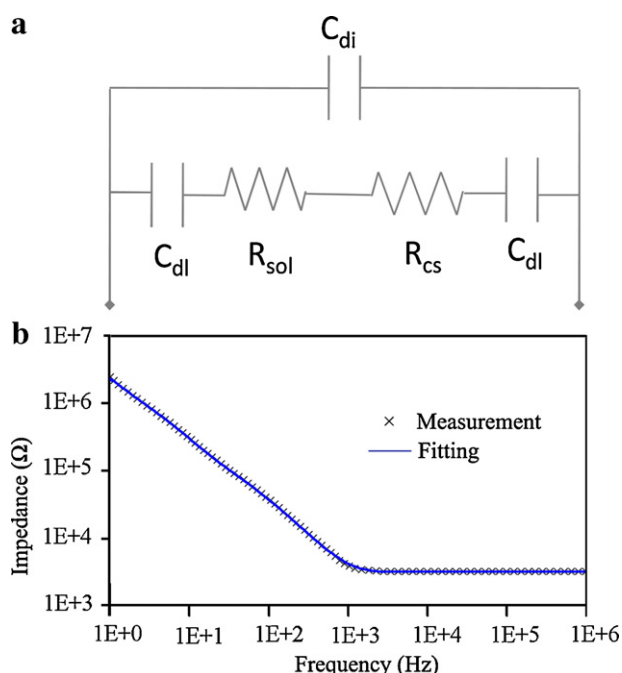


**Fig. 4.** (a) The equivalent electric circuit of the interdigitated electrodes based on immobilization of serum antibodies, where  $C_{dl}$ ,  $R_{sol}$ ,  $R_{cs}$ , and  $C_{di}$  represent the double layer capacitance, the solution resistance, the interfacial resistance of the biomolecules complex on the surface between two electrodes, and the dielectric capacitance, respectively and (b) an impedance spectrum (Bode plot) for the serum antibody-based interdigitated sensor with the fitting curve in the frequency range from 1 Hz to 1 MHz.

A and B of the Lock-in amplifier, and processed by a computer via the RS-232 interface. At low frequencies (100 Hz and 1 kHz), the differential impedance of the serum antibody-based biosensor started decreasing linearly at  $1 \mu\text{g/ml}$  JEV antigens, recognizing clearly with increase in concentration from  $10 \mu\text{g/ml}$  to  $50 \mu\text{g/ml}$ , and saturated quickly with higher concentrations of JEV antibodies. It could be that the concentration of  $1 \mu\text{g/ml}$  JEV antigens started binding to immobilized serum antibodies, and provide the physical effect on the sensor surface leading to the change in impedance of the biosensor, and that the binding probability of JEV antigens–serum antibodies became more rapid on the sensor

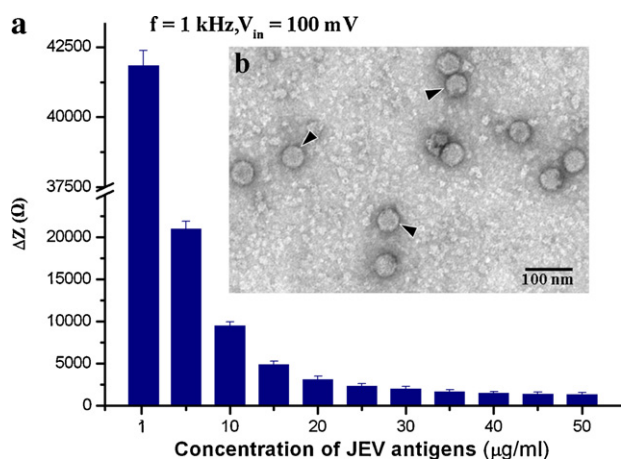


**Fig. 5.** The differential impedance of the biosensor developed obtained by immersing in different concentrations of JEV antigens at 100 mV and 1 kHz (a). JEV particles with spherical shapes and about 45 nm in diameter (arrow-heads) were found in the sample using transmission electron microscopy after ultracentrifugation (b). Error bars calculated from the mean ( $n = 5$ ).

surface with higher concentrations of JEV antigens. On the other hand, at high frequencies (10 kHz, 100 kHz and 1 MHz), little change in signal corresponding to the concentration of JEV antigens was detected (data not shown). After immersion of the serum antibody-based biosensor into the analysis solution, viral antigens become bound to the serum antibodies on the working electrodes region and form a complex of viral antigens/antibody/protein A/GA/APTES on both the electrodes surface (double capacitance layer) and the space between electrodes (interfacial resistance), resulting in the impedance change across the Pt electrodes. This change correlates with the concentration of viral antigens found in the analysis solution. This complex could result in increase in the interfacial capacitance and decrease in the interfacial resistance [38]. Moreover, at high frequencies the number of viral antigens binding to the sensor surface that would be minimized due to the relaxation of small dipole molecules, as well as by the double layer capacitance at the interface that would be minimized. At lower frequencies the current does not flow through the dielectric capacitance and the large complex of biomolecules on the sensor surface would add different impedance elements to total impedance. Whereas viral antigens could not bind specifically to the reference electrodes region due to the absence of serum antibodies immobilized. Consequently, the electrical measurements were easily obtained by the differential signal caused by the specific binding of viral antigens on the working electrode region in comparison to the non-specific bindings on the reference electrodes region. Hence, the designed configuration of this sensor is expected to minimize the influence of interfering molecules and non-specific adsorption for rapid detection of the pathogens in different types of sample such as blood, cerebrospinal fluid, and nasopharyngeal washes, even without the use of toxic redox probes such as  $[\text{Fe}(\text{CN})_6]^{4-/3-}$  [39,40].

Fig. 6 presents the group of differential voltages resulting from the change in impedance responses of the serum antibody-based biosensor corresponding to defined concentrations of viral antigens. These signals were measured at 100 mV, 1 kHz, and various concentrations of JEV antigens; Dengue antigens, and healthy mouse serum served as possible interfering molecules for the sensitivity and selectivity of the biosensor developed. While there was a minor change and quick saturation in the tests with the mouse serum diluted by 50 times (Fig. 6a;  $S_M$ ), a significant difference in the voltage of the biosensor was seen that increased with increasing JEV antigen concentrations (Fig. 5a;  $J_{10}$ ,  $J_{20}$ ,  $J_{30}$ , and  $J_{50}$ ). This indicates that the increase in the differential voltages is due to sufficient concentration of JEV antigens bound on the working electrodes in comparison with reference electrodes. Moreover, most of these tests demonstrated that the time of response required to detect JEV antigens was 5 min and was stabilized in 20 min. In other attempts, the biosensor was tested for its capacity to detect lower concentrations (less than  $10 \mu\text{g/ml}$ ) of JEV antigens. The results showed that this biosensor can detect JEV antigens, even at  $1 \mu\text{g/ml}$ . The limit of detection (LOD) was  $0.75 \mu\text{g/ml}$  estimated from the standard deviation of the measurement signals for the blank [41]. However, at this concentration, the signal obtained is not sufficiently high over the signal comes from interfering molecules of Dengue antigens (Fig. 6b). To overcome this drawback, the sensing surface of the sensor will need to be improved by reducing interdigitated micro-electrodes [42] or by using suitable materials for the signal amplification [43,44]. The detailed fitting results for Fig. 6b are shown in complementary data (Table 1A).

In fact, this study reported the development of serum antibody-based biosensor applied for rapid detection of infectious pathogens in blood samples, and the experimental data showed that the influence of serum proteins was minimal (Fig. 6a;  $S_M$ ). However, the serum antibodies should be selected and screened carefully to avoid cross-reactivities with potential pathogens in the samples tested during the measurement.

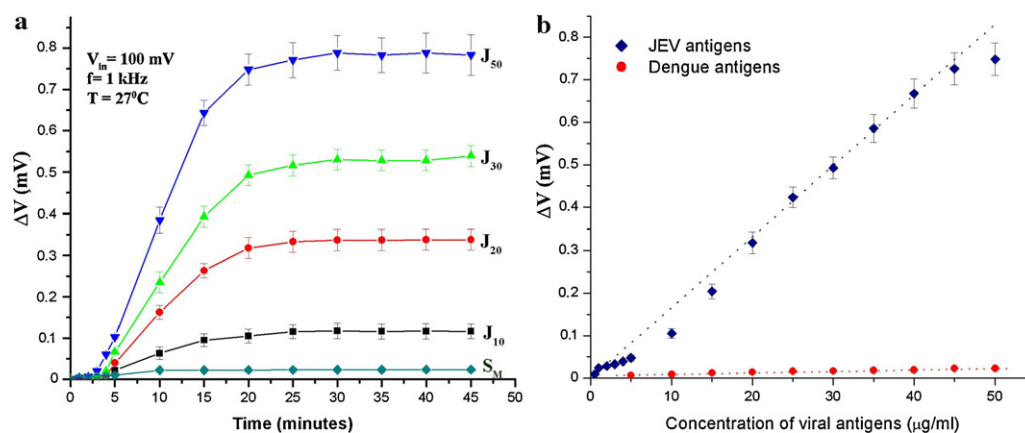


**Fig. 6.** The differential voltages of the serum antibody-based biosensor corresponding to concentrations of analytes: mouse serum diluted by 50 times ( $S_M$ ); JEV antigens: 10  $\mu\text{g/ml}$  ( $J_{10}$ ), 20  $\mu\text{g/ml}$  ( $J_{20}$ ), 30  $\mu\text{g/ml}$  ( $J_{30}$ ) and 50  $\mu\text{g/ml}$  ( $J_{50}$ ) (a). Fitting lines for the relationship between the differential voltage change and the concentration of viral antigens (b). Error bars calculated from the mean ( $n = 5$ ).

**Table 1**

Brief summary of results reported on several biosensors for the detection of viral antigens.

Techniques of detection	Probe	Analyte	Limit of detection	Detection time	Ref.
Piezoelectric	Horse polyclonal antibody	SARS-Cov	0.6–4 $\mu\text{g/ml}$	2 min	[45]
Piezoelectric	Monoclonal antibodies specific to proteins E and NS1	Dengue virus	1.727 $\mu\text{g/ml}$ (protein E) 0.74 $\mu\text{g/ml}$ (protein NS1)	Not given	[46]
Impedance spectroscopy	Specific $\text{H}_7\text{N}_1$ antibodies	A/ $\text{H}_7\text{N}_1$ Influenza virus	5 $\mu\text{g/ml}$	Not given	[47]
Impedance spectroscopy	Polyclonal HA antibody	A/ $\text{H}_5\text{N}_1$ Influenza virus	$10^3 \text{ EID}_{50}/\text{ml}$	2 h	[40]
Amperometric	HBs antibody	HBsAg	About 100 times more sensitive than ELISA	Not given	[48]
Surface plasmon resonance	Specific HA proteins	A/ $\text{H}_1\text{N}_1$ , A/ $\text{H}_3\text{N}_2$ , B Influenza virus	0.5–10 $\mu\text{g/ml}$	Not given	[49]
Square wave voltammetry	Ferrocene-labeled lipoic acid	RT-specific peptide	50 pg/ml	20 s	[20]
Non-Faradic impedance	Screened human serum antibody	JEV antigens	0.75 $\mu\text{g/ml}$	20 min	This study

$\text{EID}_{50}$ : 50% egg infective dose.

For comparison, recent results reported on several biosensors for the detection of viral antigens have been referred (see Table 1). These biosensors were developed using some transducers with different techniques of detection, and specific antiviral antibodies (purified antibodies) as probes. Although most of them showed impressive limits of detection of viral antigens, but the time required for the detection was not mostly given or discussed. It is indeed not easy to dispose of these purified antibodies, especially against unknown pathogens within a short period of time when an outbreak arises. So, the serum antibody-based biosensor revealed the convenience, the quick response to yield a result, the ease of operation, and the potential application in rapid and direct detection of viral antigens in clinical samples for preliminary pathogenic screenings in the case of possible outbreaks.

#### 4. Conclusion

We have successfully developed a label-free biosensor based on immobilizing serum antibodies and non-Faradic impedance for rapid detection of JEV antigens. The change in impedance caused by the specific binding on working electrodes compared to the non-specific reaction on reference electrodes resulted in the difference of the voltage between these two electrodes. The measurements were performed without using toxic redox probes, and were obtained by the differential voltage in the output. The analysis showed that the detection range of this biosensor was 1–10  $\mu\text{g/ml}$  JEV antigens, with a detection limit of 0.75  $\mu\text{g/ml}$  and the detection time only about 20 min. As developed serum antibody-based biosensor revealed the convenience, the quick response to yield a result, high selectivity, and a promising and powerful device for

rapid and direct detection of viral antigens as well as for preliminary pathogenic screenings in viral disease outbreaks.

#### Acknowledgments

The authors wish to thank Anne-Lise Haenni, Institut Jaques Monod/CNRS – Université Paris Diderot – Paris 7, France, for her English correction and helpful comments on the manuscript. We also thank to professor Nguyen Van Hieu, International Training Institute for Materials Science (ITIMS), Hanoi University of Science and Technology (HUST) for his helpful comments on the revised manuscript. This work was financially supported by Vietnam's National Foundation for Science and Technology Development (NAFOSTED), project code: 106.16.181.09.

#### Appendix A. Supplementary data

Supplementary data associated with this article can be found, in the online version, at doi:10.1016/j.talanta.2011.09.012.

#### References

- [1] E.K. Jones, G.N. Patel, A.M. Levy, A. Storeygard, D. Balk, L.J. Gittleman, P. Daszak, *Nature* 451 (2008) 990–993.
- [2] R.J. Coker, B.M. Hunter, J.W. Rudge, M. Liverani, P. Hanvoravongchai, *Lancet* 377 (2011) 599–609.
- [3] G. Palacios, Q. Phenix-Lan, et al., *Emerg. Infect. Dis.* 13 (2007) 73–81.
- [4] P.G. Engelkirk, J. Duben-Engelkirk, *Laboratory Diagnosis of Infectious Diseases: Essentials of Diagnostic Microbiology*, Lippincott Williams & Wilkins, 2008.
- [5] F. Kuralay, S. Campuzano, D.A. Haake, J. Wang, *Talanta* 85 (2011) 1330–1337.
- [6] S.H. Tanya, G. Supratim, G. Yali, C.W.C. Warren, *Drug Deliv. Rev.* 62 (2010) 438–448.

- [7] M.A. Alonso-Lomillo, O. Domínguez-Renedo, M.J. Arcos-Martínez, *Talanta* 82 (2010) 1629–1636.
- [8] T.G. Drummond, M.G. Hill, J.K. Barton, *Nat. Biotechnol.* 10 (2003) 1192–1199.
- [9] M.H. Shamsi, H.-B. Kraatz, *Analyst* 136 (2011) 3107–3112.
- [10] C.L. Morgan, D.J. Newman, C.P. Price, *Clin. Chem.* 42 (1996) 193–209.
- [11] M.H. Shamsi, H.-B. Kraatz, *Analyst* 135 (2010) 2280–2285.
- [12] P.M. Diakowski, H.-B. Kraatz, *Chem. Commun.* 47 (2011) 1431–1433.
- [13] M. Diakowski, H.-B. Kraatz, *Chem. Commun.* 118 (2009) 9–1191.
- [14] P.D. Tam, M.A. Tuan, T.Q. Huy, L.T. Anh, N.V. Hieu, *Mater. Sci. Eng. C* 30 (2010) 1145–1150.
- [15] M. Labib, P.O. Shipman, S. Martic, H.-B. Kraatz, *Analyst* 136 (2011) 708–715.
- [16] P.B. Lippa, L.J. Sokoll, D.W. Chan, *Clin. Chim. Acta* 314 (2001) 1–26.
- [17] B. Pejčić, R.D. Marco, G. Parkinson, *Analyst* 131 (2006) 1079–1090.
- [18] D. Bhatta, E. Stadden, E. Hashem, G.J.I. Sparrow, D.G. Emmerson, *Sens. Actuators B* 149 (2010) 233–238.
- [19] M. Labib, S. Martic, P.O. Shipman, H.-B. Kraatz, *Talanta* 85 (2011) 770–778.
- [20] M. Labib, P.O. Shipman, S. Martic, H.-B. Kraatz, *Electrochim. Acta* 56 (2011) 5122–5128.
- [21] S.M. Radke, E.C. Alocilja, *Biosens. Bioelectron.* 20 (2005) 1662–1667.
- [22] L. Yang, R. Bashir, *Biotechnol. Adv.* 26 (2008) 135–150.
- [23] P. Paul, S.W. David, et al., *Anal. Biochem.* 312 (2003) 113–124.
- [24] G. Liu, Y. Lin, *Talanta* 74 (2007) 308–317.
- [25] Z. Pei, H. Anderson, A. Myrskog, G. Dunér, B. Ingemarsson, T. Aastrup, *Anal. Biochem.* 398 (2010) 161–168.
- [26] P.D. Tam, M.A. Tuan, N.V. Hieu, N.D. Chien, *Physica E* 41 (2009) 1567–1571.
- [27] A. Sibai, K. Elamri, D. Barbier, N. Jaffrezic-Renault, E. Souteyrand, *Sens. Actuators B* 31 (1996) 125–130.
- [28] J. Kong, S. Yu, *Acta Biochim. Biophys. Sin.* 39 (2007) 549–559.
- [29] G.D. Nagare, S. Mukherji, *Appl. Surf. Sci.* 255 (2009) 3696–3700.
- [30] R.M. Pasternack, S.R. Amy, Y.J. Chabal, *Langmuir* 24 (2008) 12963–12971.
- [31] L.C. Junqueira, C. Jose, *Basic Histology*, McGraw-Hill, 2003.
- [32] A. Surolija, D. Pain, M.I. Khan, *Trends Biochem. Sci.* 7 (1982) 74–76.
- [33] I. Takeshi, H. Yumehiro, N. Ken-ichi, I. Yoshiaki, T. Keigo, A. Satoka, H. Ryuichi, K. Akio, *Anal. Biochem.* 385 (2009) 132–137.
- [34] A.K. Minkstiene, A. Ramanaviciene, J. Kirlyte, A. Ramanavicius, *Anal. Chem.* 82 (2010) 6401–6408.
- [35] G. Shen, C. Cai, K. Wang, J. Lu, *Anal. Biochem.* 409 (2011) 22–27.
- [36] T.Q. Huy, N.T.H. Hanh, P.V. Chung, D.D. Anh, P.T. Nga, M.A. Tuan, *Appl. Surf. Sci.* 257 (2011) 7090–7095.
- [37] P. Van Gerwen, W. Laureyn, W. Laureys, G. Huyberechts, M. Op De Beek, M.K. Baert, J. Suls, W. Sansen, P. Jacobs, L. Hermans, R. Mertens, *Sens. Actuators B* 49 (1998) 73–80.
- [38] X. Fang, O.K. Tan, M.S. Tse, E.E. Ooi, *Biosens. Bioelectron.* 25 (2010) 1137–1142.
- [39] L. Yang, Y. Li, G.F. Erf, *Anal. Chem.* 76 (2004) 1107–1113.
- [40] H.R. Wang, Y. Wang, K. Lassiter, B.Y. Li, B. Hargis, S. Tung, L. Berghman, W. Bottje, *Talanta* 79 (2009) 159–164.
- [41] D.A. Armbruster, T. Pry, *Clin. Biochem. Rev.* 29 (Suppl. (i)) (2008) S49–S52.
- [42] Z. Zou, J. Kai, M.J. Rust, J. Han, C.H. Ahn, *Sens. Actuators A* 136 (2007) 518–526.
- [43] L.D. Tran, D.T. Nguyen, B.H. Nguyen, Q.P. Do, H.L. Nguyen, *Talanta* 85 (2011) 1560–1565.
- [44] X.Y. Dong, X.N. Mi, B. Wang, J.J. Xu, H.Y. Chen, *Talanta* 84 (2011) 531–537.
- [45] L.B. Zuo, M.S. Li, Z. Guo, F.J. Zhang, Z.C. Chen, *Anal. Chem.* 76 (2004) 3536–3540.
- [46] Z.T. Wu, C.C. Su, K.L. Chen, H.H. Yang, F.D. Tai, C.K. Peng, *Biosens. Bioelectron.* 21 (2005) 689–695.
- [47] M.F. Diouani, S. Helali, I. Hafaid, W.H. Hassen, M.A. Snoussi, A. Ghrum, N. Jaffrezic-Renault, A. Abdelghani, *Mater. Sci. Eng. C* 30 (2008) 580–583.
- [48] C. Ding, H. Li, K. Hu, M.J. Lin, *Talanta* 80 (2010) 1385–1391.
- [49] E.C. Nilsson, S. Abbas, M. Bennemo, A. Larsson, D.M. Härmäläinen, A. Frostell-Karlsson, *Vaccine* 28 (2010) 759–766.